https://doi.org/10.1016/j.apenergy.2017.08.116

Transport phenomena in direct borohydride fuel cells

L. An[a]* and C.Y. Jung[b]*

[a] Department of Mechanical Engineering, The Hong Kong Polytechnic University, Hung Hom, Kowloon, Hong Kong SAR, China.

[b] Hydrogen & Fuel Cell Center, New & Renewable Energy Research Division, Korea Institute of Energy Research, Republic of Korea.

*Corresponding authors.

[a] E-mail: liang.an@polyu.edu.hk (L. An)

[b] E-mail: cyjung@kier.re.kr (C.Y. Jung)

Abstract

Direct borohydride fuel cells, which convert the chemical energy stored in borohydride directly into electricity, are one of the most promising energy-conversion devices for portable, mobile and stationary power applications, primarily because they run on a carbon-free fuel and uses the low-cost materials. For this reason, this energy technology has undergone a rapid progress over the last decade. This article provides a comprehensive review of transport phenomena of various species in direct borohydride fuel cells. Particular attention is paid to the understanding of the critical issues related to transportation of various species through the fuel cell structure.

Keywords: Fuel cells; Direct borohydride fuel cells; Membrane electrode assembly; Transport phenomena; Two-phase flow

1. Introduction

Alkaline direct oxidation fuel cells (DOFC) running on various fuels have received ever-increasing attention, mainly due to increased performance as a result of fast electrochemical kinetics at both the anode and cathode in alkaline media [1-5]. Among the fuels used, borohydride has been recognized as one of the most suitable fuels as it is a carbon-free fuel and possesses many unique physicochemical properties including high energy density and ease of transportation and storage as well as handling [6-10]. Direct borohydride fuel cell, using an anion exchange membrane (AEM), was demonstrated by Amendola et al. [6] and resulted in a peak power density of 60 mW cm^{-2} at 70^{o}C, in which the architecture design was similar to that in polymer electrolyte membrane fuel cells (PEMFC). The alkaline environment not only alleviates the hydrolysis of borohydride to hydrogen, but also allows us to use non-precious-metal or even non-metal electrocatalysts. For these reasons, tremendous efforts have been made to the development of direct borohydride fuel cells over the past decade [11-30]. It should be mentioned that the oxidation product of borohydride, borate, can be converted back to borohydride via many approaches [11], although there exist some technical issues associated with this conversion process [22-25]. Generally, an alkali, MOH (e.g.: NaOH/KOH), is added to the fuel solution to stabilize the borohydride, as borohydride can be decomposed into hydrogen and BO_2^-

in the aqueous solution. The involvement of an alkali further upgrades the fuel cell performance, due to the fact that it not only allows a drastic increase in the ionic transport rate through the membrane [31-35], but also enables the kinetics of the electrochemical reactions to be speeded up [36-40]. As such, the co-presence of M^+, BH_4^-, BO_2^- and OH^- ions in the present fuel cell system creates an anion-cation co-existing system, thereby showing more complicated transport phenomena [41, 42]. The past review articles regarding direct borohydride fuel cells are mainly focused on electrocatalysts and their preferred mechanisms for BOR and ORR in alkaline media [43, 44, 45], membranes and separators [46, 47], as well as fuel cell performance comparison [48, 49, 50]. This article provides a review of the past research on transport phenomena of various species through the fuel cell structure.

2. System description

The direct borohydride fuel cell structure is borrowed from the PEMFC that is composed of an anode flow field, an anode diffusion layer (DL), an anode catalyst layer (CL), an AEM or a cation exchange membrane (CEM), a cathode CL, a cathode DL and a cathode flow field, as shown in Fig. 1a.

AEM-based direct borohydride fuel cells: on the anode, borohydride will be oxidized to generate electrons, water, and borate [46]:

$$\mathrm{NaBH_4} + 8\mathrm{OH^-} \rightarrow \mathrm{NaBO_2} + 6H_2O + 8\mathrm{e^-} \qquad \mathrm{E}_a^o = -1.24V\ vs.SHE \tag{1}$$

It should be noted that an issue associated with the use of borohydride in fuel cells is the hydrolysis of borohydride ions (BH_4^-) to hydrogen [46]:

$$NaBH_4 + 2H_2O \rightarrow NaBO_2 + 4H_2 \quad (2)$$

The hydrogen evolution will lower the utilization efficiency of borohydride and cause a two-phase counterflow that increases the transport resistance of liquid reactants. On the cathode, oxygen combines with electrons and water to produce OH^- ions [34]:

$$O_2 + 2H_2O + 4e^- \rightarrow 4OH^- \qquad E_c^o = 0.4V\ vs.SHE \quad (3)$$

Subsequently, the generated OH^- ions are conducted through the AEM to the anode for the BOR.

CEM-based direct borohydride fuel cells: as sodium hydroxide is added to the anolyte solution, cations Na^+ will be present at the anode:

$$12NaOH \rightarrow 12Na^+ + 12OH^- \quad (4)$$

The presence of cations Na^+ at the anode leads to think that it is also possible to use a CEM to conduct cations Na^+ from the anode to cathode [51, 52], as shown in Fig. 1b. Regardless the membrane type (AEM or CEM), combining the BOR given by Eq. (1) and the ORR given by Eq. (3) results in an overall reaction [46]:

$$NaBH_4 + 2O_2 \rightarrow NaBO_2 + 2H_2O \qquad E^o = 1.64\ V \quad (5)$$

In addition, hydrogen peroxide (H_2O_2) has recently received increasing attention as an alternative oxidizer, primarily due to several advantageous characteristics in

comparison to gaseous oxygen, such as operation in an oxygen-free environment (outer space and underwater). For this reason, much effort has been devoted to developing fuel cells that can use hydrogen peroxide as an oxidant and significant progress has been made [53-59]. It should be noted that the hydrogen peroxide reduction reaction (HPRR) strongly depends on the electrolyte used. In alkaline media, hydrogen peroxide exists in the form of HO_2^- [60]:

$$H_2O_2 + OH^- \rightarrow HO_2^- + H_2O \tag{6}$$

Hydrogen peroxide reacts with water and electrons to form hydroxyl ions [60]:

$$HO_2^- + H_2O + 2e^- \rightarrow 3OH^- \qquad E_{c,1}^0 = 0.87\,\text{V vs.SHE} \tag{7}$$

In acid media, when hydrogen peroxide is adsorbed on the electrode, the HPRR will take place by combining protons and electrons to form water [60]:

$$H_2O_2 + 2H^+ + 2e^- \rightarrow 2H_2O \qquad E_{c,1}^0 = 1.78\,\text{V vs.SHE} \tag{8}$$

where $E_{c,1}^0$ represents the standard electrode potential of the HPRR. It should be noted that hydrogen peroxide oxidation reaction (HPOR) can easily take place in both alkaline and acid media at such a high potential to release oxygen, protons and electrons, respectively [60]:

$$H_2O_2 \rightarrow O_2 + 2H^+ + 2e^- \qquad E_a^0 = 0.69\,\text{V vs.SHE} \tag{9}$$

$$HO_2^- + OH^- \rightarrow O_2 + H_2O + 2e^- \qquad E_a^0 = 0.15\,\text{V vs.SHE} \tag{10}$$

It can be seen that in acid or alkaline media, therefore, one is an oxidation reaction,

and the other is a reduction reaction. As such, a redox reaction occurs on one electrode, forming a so-called mixed potential. It is known that the formation of the mixed-potential phenomenon not only significantly lowers the electrode potential and thus decreases the cell voltage, but also causes the electrochemical decomposition of hydrogen peroxide that lowers the utilization efficiency. Detailed discussion related to the mechanisms of mixed potential formed in hydrogen peroxide fuel cells can be found in the previous review paper [60]. It also should be noted that the presence of both cations (M^+) and (BH_4^-, BO_2^- and OH^-) ions creates an anion-cation co-existing system, thereby showing more complicated transport phenomena. In the following sections, we discuss the transport characteristics of various species and review the past investigations with regard to the transport phenomena.

3. Transport phenomena in the anode

In the anode, borohydride in the fuel solution flowing into the anode flow channel is transported through the anode DL to the anode CL. Simultaneously, the gaseous hydrogen released via the hydrolysis of borohydride has to be removed from the anode. Thus, the formation of the two-phase counterflow increases the transport resistance of borohydride to the active sites. For this reason, the operating and structural design parameters can affect the transportation of borohydride in the anode. A low local concentration of borohydride will increase the potential loss due to the

increased resistance and thus lower the anode performance. On the other hand, a high local concentration will increase the rate of the borohydride crossover, which results in a serious mixed-potential problem at the cathode and a waste of fuel. Hence, it is critically important to maintain an appropriate local borohydride concentration and speed up the removal rate of hydrogen.

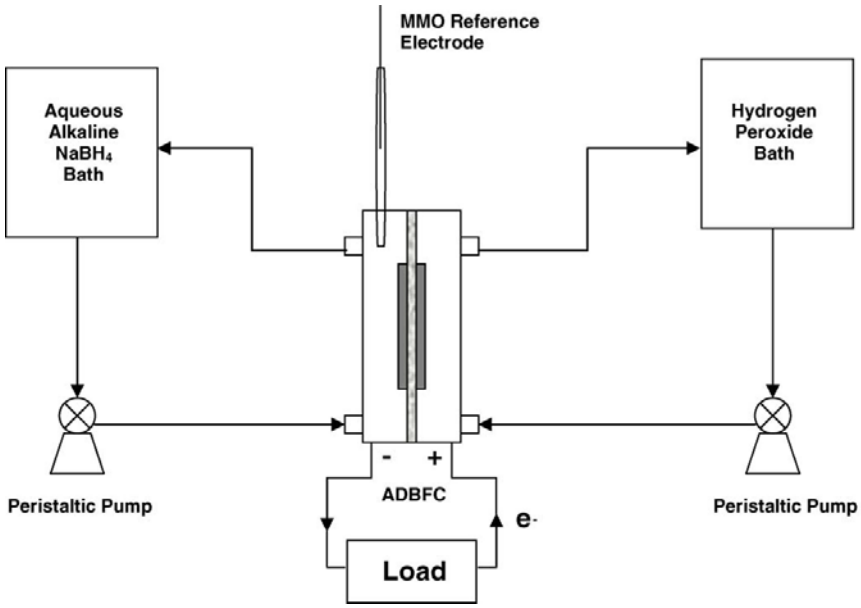

Fig. 2 Schematic of an alkaline direct borohydrides fuel cell operating with hydrogen peroxide as oxidant [61].

3.1. Effect of the borohydride concentration in the fuel solution

The initial borohydride concentration in the fuel solution is an important parameter that can affect the local borohydride concentration. Hence, the effect of the initial borohydride concentration on the cell performance has been extensively studied [61-72]. For example, Choudhury et al. [61] developed and fabricated an alkaline direct borohydride fuel cell that uses hydrogen peroxide as oxidant and sodium

borohydride as fuel, as shown in Fig. 2. They optimized the $NaBH_4$ concentration ranging from 5 wt. % to 20 wt. % in the fuel solution (containing 20 wt. % NaOH) at a flow rate of 3.0 mL min^{-1} when the cathode was fed with a fixed concentration of hydrogen peroxide (8.9 M) at a flow rate of 5.0 mL min^{-1} and found that 10 wt. % $NaBH_4$ in the fuel solution resulted in the highest peak power density. Cao et al. [62] developed and fabricated an alkaline direct borohydride/hydrogen peroxide fuel cell using Pt-Ru catalyzed nickel foam as the anode and Pd-Ir catalyzed nickel foam as the cathode. They also investigated the effect of the borohydride concentration ranging from 0.1 M to 0.5 M in the fuel solution (containing 3.0 M NaOH) on the cell performance and found that the performance was nearly independent of the borohydride concentration when higher than 0.2 M, as shown in Fig. 3. It was also found that the highest peak power density (198 mW cm^{-2}) was achieved when operated with 0.4 M $NaBH_4$ at room temperature. Duteanu et al. [65] reported a direct borohydride fuel cell, which was fabricated with an AEM, Pt-Ru/C as the anode electrocatalyst and Pt/C as the cathode electrocatalyst. It was found that when the borohydride concentration was increased from 1.0 M to 2.0 M, the peak power density was also increased from 150 mW cm^{-2} to 200 mW cm^{-2} at 60°C. Celik et al. [70] systematically investigated the effects of the sodium borohydride concentration (0.5 M, 1.0 M and 1.5 M) on the performance of a direct borohydride fuel cell, which

was constructed with the Pd/C electrocatalyst as anode, the Pt/C electrocatalyst as cathode, and Na^+ conducting membrane (Nafion) as the solid electrolyte. They found that the peak power density was increased with increasing the sodium borohydride concentration for steady state/steady-flow system, while the peak power density was decreased with increasing the sodium borohydride concentration for uniform state/uniform-flow system. It was explained that the decreased performance was mainly attributed to the increased fuel crossover rate and hydrogen generation rate.

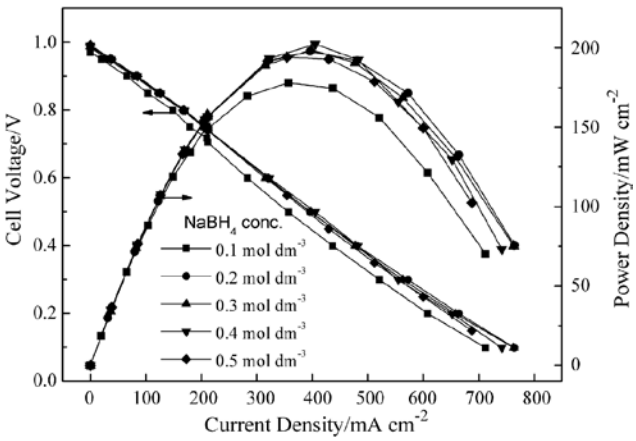

(a)

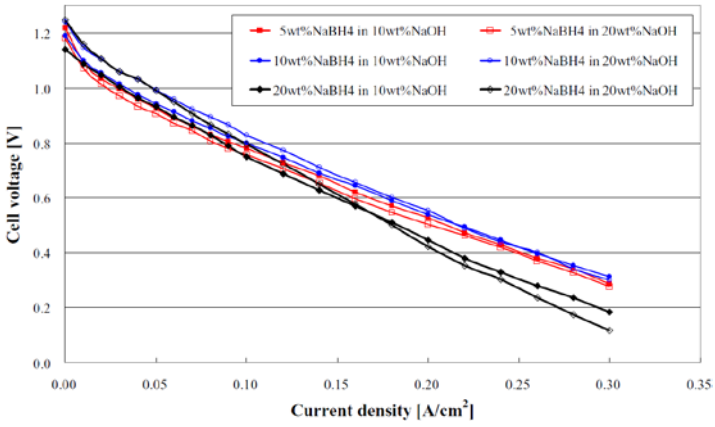

(b)

Fig. 3 (a) Effect of the borohydride concentration on the cell performance [62]; (b)

effect of the alkali concentration on the cell performance [64].

In summary, an increase in the initial borohydride concentration can increase the delivery rate of borohydride to the active sites. When the local borohydride concentration is too high, however, most of active sites are occupied by borohydride and thus the adsorption of hydroxide ions on the active sites is limited. The mismatch between borohydride-ion and hydroxide-ion concentrations on the reaction sites lowers the anodic kinetics and thus decreases the anode performance. On the other hand, too high local borohydride concentration results in a high crossover rate of borohydride, causing a serious mixed-potential problem and thus lowering the cathode performance. Therefore, there exists an optimal initial borohydride concentration at which the fuel cell results in the best performance.

3.2. Effect of the alkali concentration in the fuel solution

The initial alkali concentration in the fuel solution is also an important parameter that can affect the anodic reaction and thus the cell performance. Hence, the effect of the alkali concentration in the fuel solution on the cell performance has been extensively studied [61, 64-68, 71, 73-76]. For example, Li et al. [64] investigated the effect of alkali concentration (10 wt. % and 20 wt. %) in the fuel solution on the cell performance of a direct borohydride fuel cell, as shown in Fig. 3b. It is well known that an increase in the alkali concentration is favorable to the anodic reaction. They

found that the cathode potential was decreased in a linear fashion with the NaOH concentration; while the anode potential was almost unchanged. An increase in the NaOH concentration led to an increase in the viscosity of the solution and thus an increase in the ohmic loss, particularly at higher current densities. Celik et al. [73] constructed a direct borohydride fuel cell using the Pd/C electrocatalyst as anode, the Pt/C electrocatalyst as cathode and Na^+ conducting membrane (Nafion) as the solid electrolyte. They also investigated the effects of various operating parameters, such as operating temperature, sodium hydroxide concentration, and electrocatalyst loading on the cell performance, and found that the optimal NaOH concentration was 20 wt. %. Specifically, the power density was increased with the sodium hydroxide concentration from 10 wt. % to 20 wt. % due to increasing the ionic conductivity of the solution and decreasing the hydrolysis rate of borohydrides. A further increase to 30 wt. % in the sodium hydroxide concentration decreased the power density due to increasing the viscosity of the solution and decreasing the mobility of charge carrier (Na^+ ions). Santos et al. [71] fabricated two direct borohydride/hydrogen peroxide fuel cells and investigated the effects of various operating parameters on the cell performance, including the fuel ($NaBH_4$ + NaOH) and oxidant (H_2O_2 + HCl) compositions, as well as the operating temperature. One was assembled by using Pt as anode and cathode separated by a Nafion 117 membrane; the other was assembled by

using Pt as anode and Prussian Blue coated Pt as cathode, which were separated by a Nafion 117 membrane. They investigated the effect of the NaOH concentration ranging from 1.0 M to 8.0 M in the fuel solution and found that an increase from 1.0 M to 4.0 M resulted in a significant increase in the peak power density; while, a further increase from 4.0 M to 8.0 M slightly upgraded the polarization curve.

In summary, on one hand, an addition of alkali can alleviate the hydrolysis rate of borohydrides, thereby limiting the hydrogen evolution rate. On the other hand, the involvement of an alkali can further improve the anodic kinetics and thus upgrade the anode performance. An increase in the initial alkali concentration can lead to an increase in the anodic reaction rate and thus improve the cell performance. However, too high alkali concentration will cause a high viscosity of the fuel solution, much lowering the effective diffusivity of borohydride ions and thus increasing the transport resistance of borohydride. In addition, too high alkali concentration will also cause the majority of the reactions sites occupied by hydroxide ions, mismatching two reactants and thus lowering the anodic kinetics. For these reasons, there also exists an optimal alkali concentration in the fuel solution at which the fuel cell results in the best performance.

3.3. Effect of the additive to the fuel solution

Adding an additive into the fuel solution may stabilize borohydrides, reducing the

hydrolysis rate of borohydrides and thus the hydrogen evolution rate, and decrease the borohydride crossover rate as a result of the ion complex formed between borohydride ions and the additive. For this reason, the effect of the additive to the fuel solution on the gas evolution rate and the cell performance has been investigated [77-80]. For example, Qin et al. [80] investigated the effects of the hydrazine addition to the fuel solution on the gas evolution and performance of a direct borohydride fuel cell. It was found that gas evolution behaviors were affected by the types of electrocatalyst and the concentrations of the fuel ($NaBH_4$) and the additive (N_2H_4). It was also found that adding hydrazine into the fuel solution could suppress gas evolution and improve the cell performance, as shown in Fig. 4.

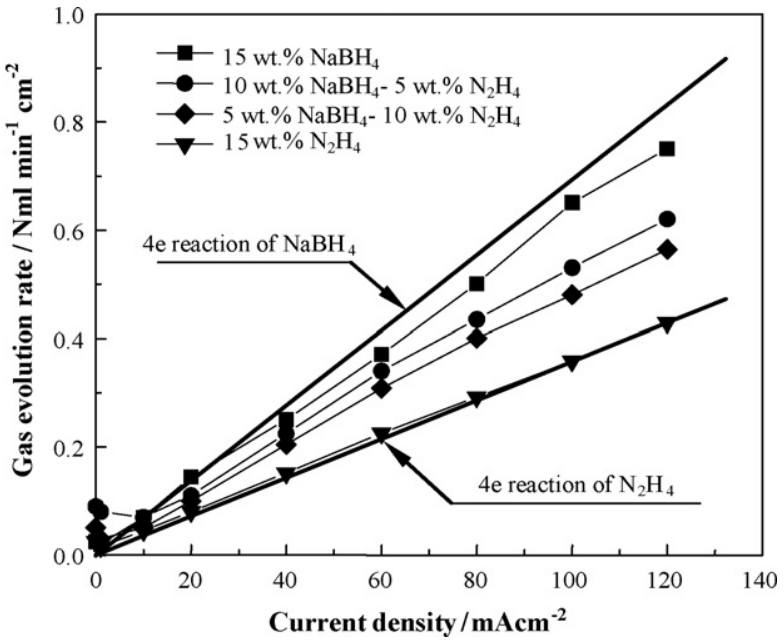

(a)

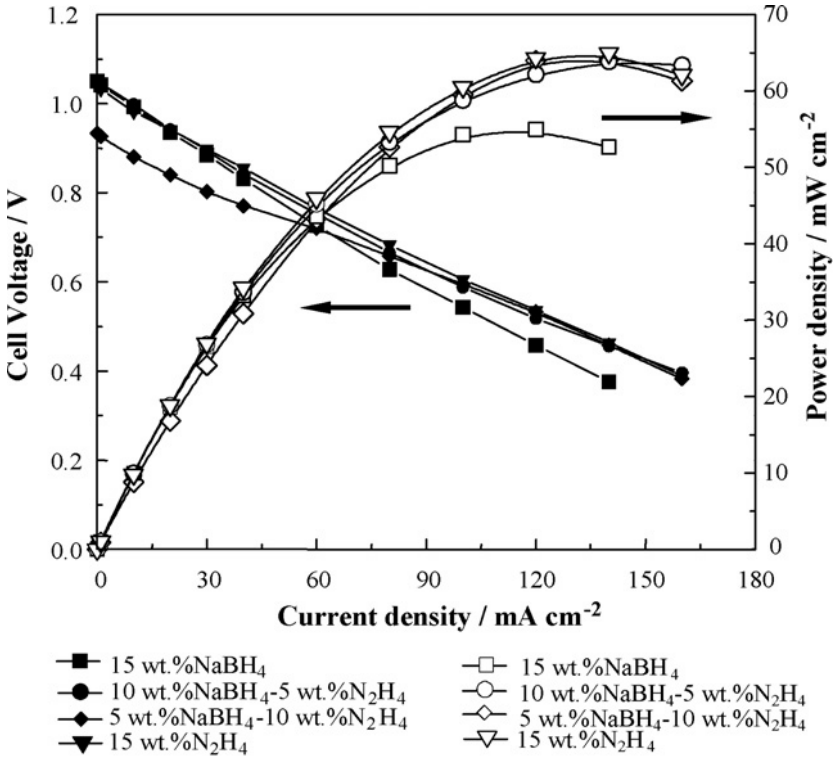

(b)

Fig. 4 Effect of the additive on (a) the gas evolution and (b) the cell performance [80].

It was also found that the gas evolution rates were first decreased and then increased linearly with the current density. In addition, the gas evolution rate was decreased with increasing the percentage of hydrazine in the fuel solution. Qin et al. [77] also investigated the effect of the additive on the cell performance and found that the power density was increased with adding the additive. They explained that the addition of hydrazine could stabilize borohydride ions in the fuel solution and form an ion complex between hydrazine and borohydride ions, decreasing the borohydride crossover rate and thus improving the cell performance. Celik et al. [78] investigated the effects of the additive, thiourea (TU), to the fuel solution under steady

state/steady-flow and uniform state/uniform-flow systems to minimize the hydrogen evolution rate on Pd. The fuel cell was fabricated with the Pd/C electrocatalyst as anode and the Pt/C electrocatalyst as cathode, which was separated by a Na^+ conducting membrane (Nafion) as the solid electrolyte. It was found that the peak power density and fuel utilization ratio were improved by an addition of TU (1.6 mM) into the fuel solution. Specifically, two cells operated with and without an addition of TU resulted in the peak power densities of 14.4 mW cm^{-2} and 15.1 mW cm^{-2}, and the fuel utilization ratios of 21.6% and 23.2%, respectively. In summary, adding an additive into the fuel solution is an effective approach to alleviate the hydrolysis of borohydride.

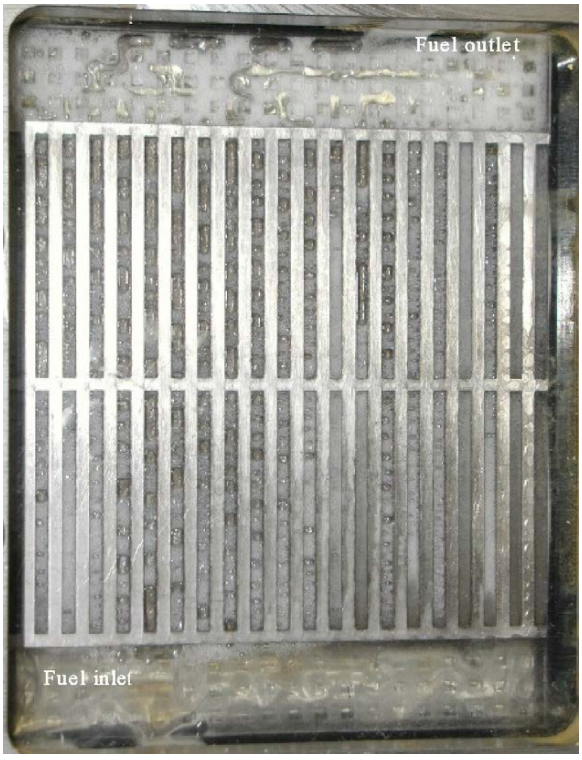

(a)

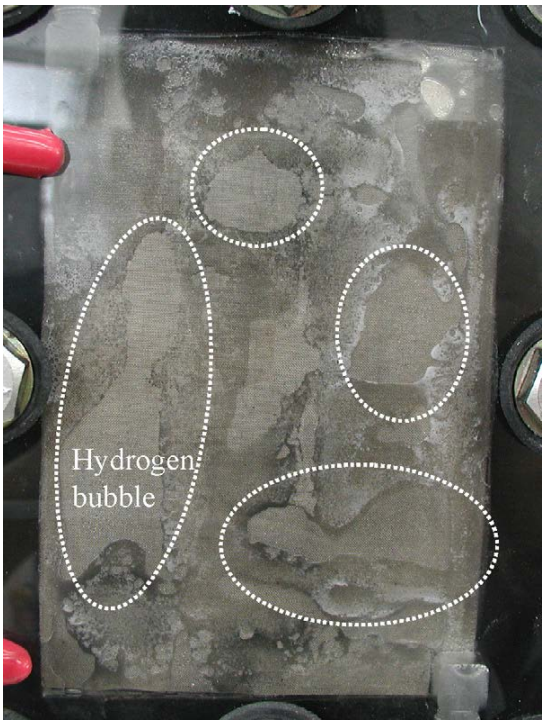

(b)

(c)

Fig. 5 (a) Visualization photo of anode channel when active hydrogen generation occurs; (b) photograph of anode when hydrogen bubbles are held in narrow gap between anode and acrylic end-plate; (c) Photograph of corrugated anode [81].

3.4. Effect of the hydrogen evolution (borohydride hydrolysis)

The hydrolysis of borohydride leads to the hydrogen evolution, forming a two-phase counterflow in the anode porous structure and a complex two-phase flow in the anode flow channel. In practice, the gas evolution may cause pressure fluctuations in the anode channel, which will induce unstable system operation and local failure of the fuel supply [81]. On one hand, the hydrolysis rate of borohydride can be slightly reduced by creating an alkaline environment via an addition of alkali in the fuel solution. On the other hand, how to effectively remove the gas bubbles is still a critically important issue. Kim et al. [81] conducted a visualization study on the two-phase flow in the anode channel of a direct borohydride fuel cell. It was observed that the slug flow was formed in the anode flow channel, increasing the transport resistance of borohydride from the channel to the active sites, as shown in Fig. 5a. They also mentioned that the hydrogen evolution decreased the rate of the anodic reaction, because the active sites were partially occupied by gas bubbles. In addition, they also designed an experimental setup to investigate the effect of the hydrogen bubbles on the cell performance, particularly for the part of which were trapped in the narrow gap (2 mm) between the membrane and the anode. Radically different from the phenomenon in the anode flow channel, it was found that large stationary hydrogen bubbles existed between the anode and the transparent end-plate, and they did not move even though the fuel pump was continuously operated, as shown in Fig.

5b. For this reason, it was inferred that there were also such stationary large bubbles trapped between the membrane and the anode, thereby forming a dead zone during operation. They also mentioned that those hydrogen bubbles in the gap could not be removed, because the gap was too narrow (2 mm) and thus the pumping pressure could not overcome the surface tension to discharge the bubbles. As such, the stationary hydrogen bubbles trapped between the membrane and the anode acted as a resistance for the charge-carrier migration through the membrane by dramatically reducing the effective area. They also found that this problem could be solved by using a corrugated anode design, which has a 2-mm gap between the membrane and the anode by forming valleys for effective evacuation of hydrogen bubbles, as shown in Fig. 5c. Liu et al. [82] constructed a 10-cell stack and a 20-cell stack of direct borohydride fuel cells, as shown in Fig. 6a. It was found that the loss of the direct borohydride fuel cell stack was mainly caused by hydrogen evolution, which led to an uneven fuel distribution in each cell of the stack. In addition, they also found that the negative effect of hydrogen evolution on the stack performance could be alleviated by changing fuel supply manner, as shown in Fig. 6b. It was demonstrated that the maximum power of the 10-cell stack reached up to 229 W. They suggested that the ultimate solution to hydrogen evolution problem is to find the anode electrocatalysts that enable the complete oxidation of borohydride ions but disable the hydrolysis of

borohydride. Similarly, Celik et al. [70] also concluded that hydrogen bubbles were easily accumulated between the membrane and the anode, thereby reducing the anodic reaction rate and increasing the ohmic loss due to blocking the charge-carrier migration through the membrane. Duteanu et al. [65] reported a direct borohydride fuel cell fabricated with an AEM, Pt-Ru/C as the anode electrocatalyst and Pt/C as the cathode electrocatalyst. It was found that the hydrogen evolution phenomenon became more severe at higher current densities. They explained that the local pH at the anode was gradually decreased due to the fact that OH^- ions were continuously consumed by the anodic reaction, consequently facilitating the hydrolysis of borohydrides to hydrogen. In fact, the severe borohydride hydrolysis at high current densities may also be caused by other reaction pathways [26-28]. In addition, the hydrolysis rate of borohydride can be decreased through optimization of the operating temperature and the fuel composition [70]. Moreover, an alternative effective approach is to develop the anode electrocatalysts that can alleviate the hydrolysis of borohydride. Li et al. [83] investigated the hydrogen evolution behaviors and the relations between hydrogen evolution rates and applied current in a direct borohydride fuel cell. It was found that hydrogen evolution rate was lowered by adding Pd, Ag and Au into electrocatalysts as the anode, and the use of a thin Nafion film coated electrocatalysts also decreased the hydrogen evolution rate. In addition, it was also

found that hydrogen evolution during the cell operation could be effectively depressed by decreasing the amount of isolated electrocatalysts, lowering the borohydride concentration on the active sites, as well as finding electrocatalysts that enable an eight-electron-transfer process. As for the addition of Nafion, the hydrogen evolution rate could be decreased in similar manners, but adding too much Nafion degraded the cell performance. Moreover, operating the fuel cell at low temperatures was also an effective way to reduce hydrogen evolution rate, but may sacrifice the fuel cell performance. In summary, the borohydride hydrolysis issue has been extensively investigated and partially addressed. The final solution may be a combination of improvements on the anode electrocatalysts, the fuel composition, as well as the electrode structural design.

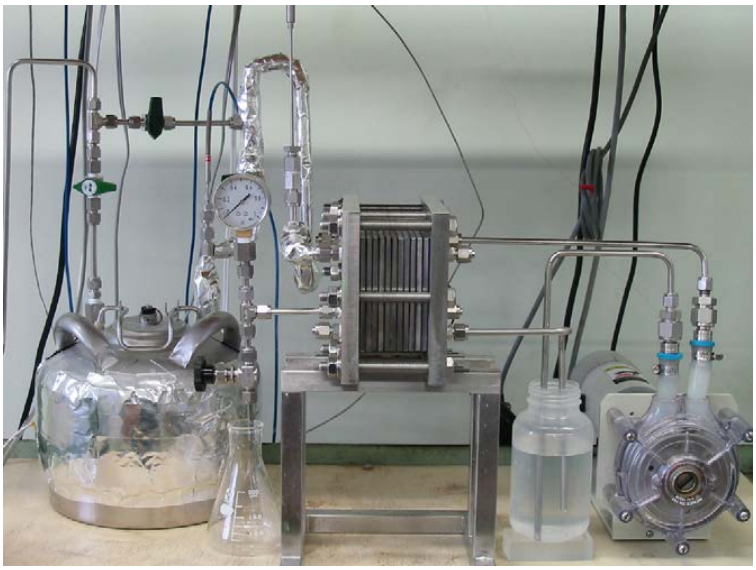

(a)

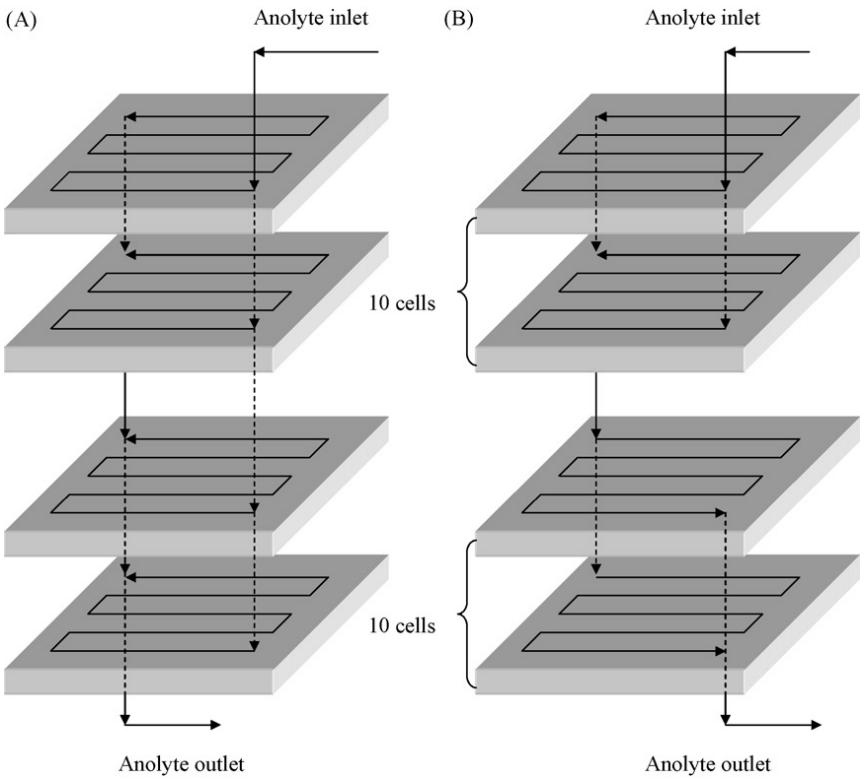

(b)

Fig. 6 (a) Direct borohydride fuel cell stack measurement set-up; (b) fuel supplies in the 20-cell stack: (left) parallel supply and (right) divided parallel supply [82].

3.5. Effect of the anolyte flow rate

For fuel cells with an active mode, the flow rate of the fuel solution can also affect the delivery rate of borohydrides to the active sites. In addition, increasing the flow rate can also speed up the removal rate of hydrogen and thus the transport of borohydride can be correspondingly enhanced. Hence, the effect of the flow rate of the fuel solution on the cell performance has been extensively studied [74, 81]. For example, Cheng et al. [74] investigated the flow rate of the fuel solution on the performance of a direct borohydride fuel cell. It was found that by using a parallel flow field, the

performance was increased by 5% in the flow rate ranging from 5 mL min^{-1} to 10 mL min^{-1}, while a further increase to 100 mL min^{-1} in the flow rate resulted in an increase in the power density by 3.5%. They explained that the higher flow rate facilitated the transport of the fuel and alleviated channel blocking and product accumulation, thereby improving the cell performance. Similarly, Kim et al. [81] investigated the effect of the flow rate of the fuel solution ranging from 25.3 mL min^{-1} to 108.4 mL min^{-1} on the cell performance. It was found that the flow rate of the fuel solution was changed from 25.3 mL min^{-1} to 53 mL min^{-1}, the peak power density was increased by 2.5%; while, a further increase to 108.4 mL min^{-1} in the flow rate decreased the cell performance. They also found that for a fuel cell stack, a low flow rate increased the stack temperature as a result of the heat generation from the losses in the physiochemical processes, thereby increasing the cell performance. In summary, an increase in the flow rate of the fuel solution can enhance the transport of borohydride in both the in-plane and through-plane directions, as well as accelerate the removal of hydrogen in the anode flow channel.

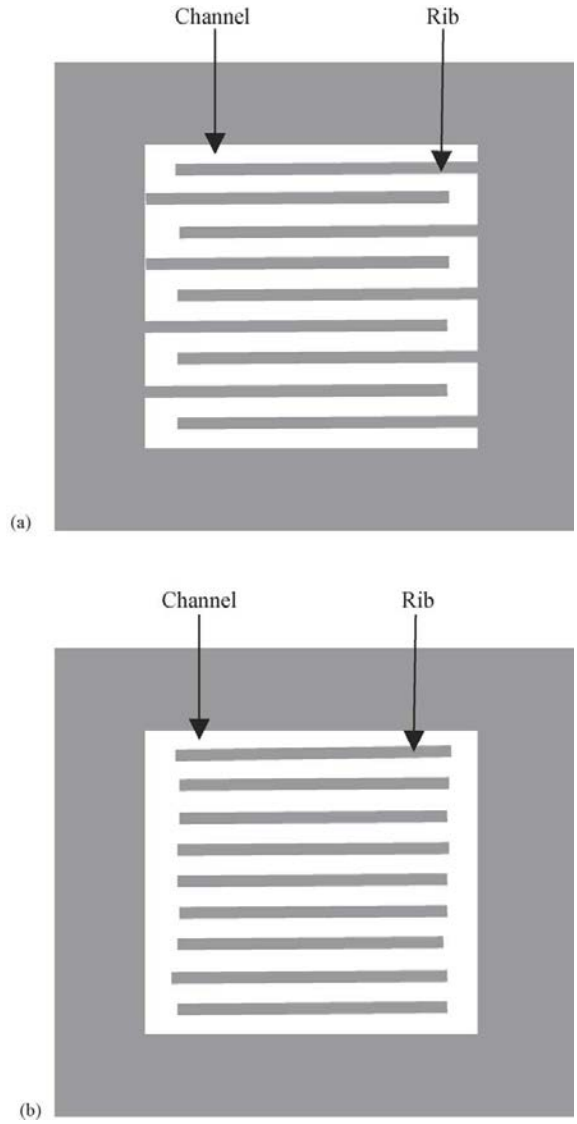

Fig. 7 Flow fields: (a) serpentine (SFF) and (b) parallel (PFF) [74].

3.6. Effect of the flow-field pattern

Generally, there are two types of flow-field pattern for fuel cells, i.e., parallel (PFF) and serpentine (SFF). In principle, the SFF offers better mass transport than the PFF, due to the fact that under the same conditions, the flow rate of the fuel solution in SFF is much higher than that in PFF. Detailed information related to the flow-field patterns for the electrochemical energy systems, such as fuel cells and flow batteries, can be

found in [85-87]. Cheng et al. [74] investigated the effect of the flow fields on the performance of a direct borohydride fuel cell. Two types of flow field, PFF and SFF, were investigated, as shown in Fig. 7a and 7b. They found that at the ambient pressure, the SFF exhibited better performance (3.5% in the peak power density) than the PFF did; while, at 1 bar pressure, the difference became smaller, even at high current densities. They also mentioned that the flow-field design was related to delivery of the reactants and removal of the products. The insignificant effect of the flow field on the direct borohydride fuel cell performance indicated that the mass transport limitation in the direct borohydride fuel cell was not serious. Kim et al. [81] designed a parallel-type flow channel for the anode of a direct borohydride fuel cell to minimize the pressure loss. They found that the pressure loss at the anode was irregularly changed with time and large fluctuations appeared. In addition, a negative pressure loss was found, indicating a back flow of the fuel solution. They concluded that the pressure loss increasing up to 20 kPa was acceptable for a general pumping pressure so that the parallel-type flow channel was effective for a direct borohydride fuel cell. In summary, the serpentine flow field is widely used due to the fact that it enhances the mass transport.

3.7. Effect of the anode structural design

In addition to the above-mentioned operating parameters, the transport process of

borohydride can also be influenced by the structural design parameters, including a porous DL and a porous CL. The previous investigations suggested the anode structure that integrates a DL and a CL was more suitable for the fuel-electrolyte-fed fuel cells than the conventional design with distinct DL and CL [88-90]. For this reason, many efforts have been made to the development of the integrated electrodes for direct borohydride fuel cells [17, 18, 88-92].

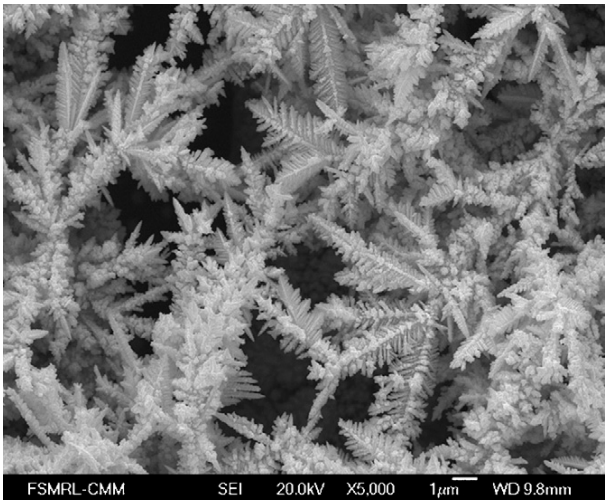

(a)

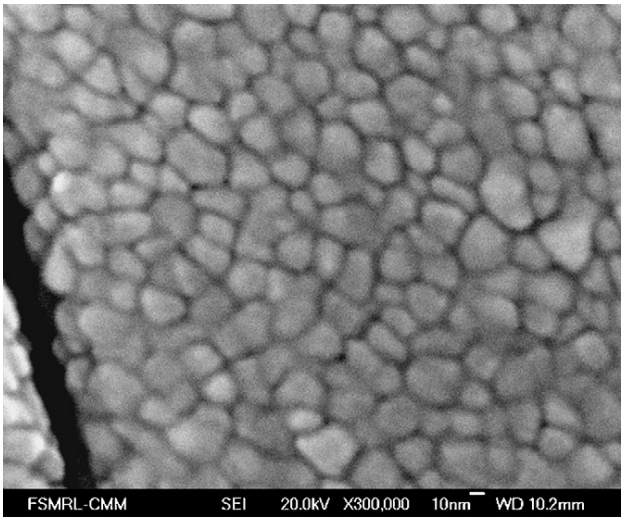

(b)

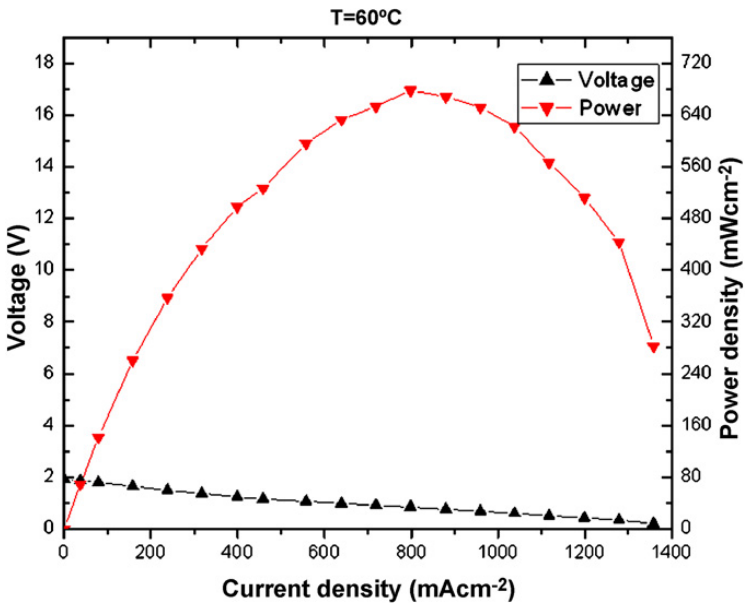

(c)

Fig. 8 (a) SEM image of Au deposits using electrodeposition method; (b) SEM image of Au deposits using sputtering method; (c) V-I and P-I curves generated by electrodeposited gold catalyst layer and electrodeposited palladium layer at 60°C [89].

Electrodeposition and sputtering are two popular methods for depositing nanoparticles on the supporting materials. For example, Miley et al. [88, 89] fabricated the metal nanoparticles onto the skeleton of the activated carbon cloth via electrodeposition and plasma sputtering deposition. It was found that as compared to the conventional method, both methods provided much higher power densities. Particularly, the sputtering method allowed a much lower catalyst loading and well-dispersed nanoparticles. It was demonstrated that by using these techniques, a direct borohydride/hydrogen peroxide fuel cell, which employed palladium as the anode electrocatalyst and gold as the cathode electrocatalyst, resulted in a peak power

density of 680 mW cm^{-2} at 60^{o}C, as shown in Fig. 8. Similarly, Cheng et al. [90] developed titanium mesh supported gold and silver anodes for direct borohydride fuel cells via thermal decomposition and electrochemical deposition. It was found that by using the developed anodes, the power density was improved up to 20% higher than those achieved by using carbon supported anodes. In summary, like other types of fuel-electrolyte-fed fuel cells, the anode structure that integrates a DL and a CL is indeed more suitable than the conventional design with distinct DL and CL.

4. Transport phenomena through the membrane

An ion exchange membrane has to be employed in fuel cells to separate the anode and the cathode, and conduct charge-carrier ions from one electrode to the other [93]. In addition to charge-carrier ions, most of the membranes are also permeable to other species in the fuel solution, including borohydrides, alkali and water in this fuel cell system. The following subsections will discuss the transport phenomena of various species through the membrane and their effects on the cell performance.

4.1. Borohydride transport through the membrane (borohydride crossover)

Borohydride transporting through the membrane (borohydride crossover) may introduce two technical issues. First, borohydride may be oxidized on the cathode to form the parasitic current, lowering the cathode performance. Second, the borohydride crossover definitely leads to a waste of fuel, lowering the utilization

efficiency of the fuel. For these reasons, the rate of borohydride crossover has to be reduced [94]. Generally, there are three transport mechanisms for borohydride crossover through the membrane, i.e., diffusion driven by the concentration gradient, electro-osmotic drag (EOD) driven by the charge-carrier migration, and convection driven by the liquid pressure gradient. It has been demonstrated that species crossover is strongly dependent of the mechanism of diffusion across the membrane in alkaline fuel cells [95]. As such, the species crossover rate mainly depends on the concentration gradient through the membrane as well as species permeability and thickness of the membrane. For this reason, the borohydride crossover rate can be reduced by lowering the concentration gradient of borohydrides through the membrane, decreasing the borohydride permeability of the membrane, but increasing the membrane thickness. Particularly, the Na^+ conducting membrane are generally used in this fuel cell system, due to the fact that the use of Na^+ conducting membrane is expected to prevent the borohydride anion crossover and show better mechanical and chemical stabilities in strong alkaline environment. For example, Li et al. [52] constructed a direct borohydride fuel cell that employs the Nafion membrane. It was found that the Nafion 117 membrane showed a high transport resistance of borohydrides. However, Lakeman [79] reported that the crossover rate of borohydride anion through the Nafion 117 membrane was 0.4×10^{-6} mol cm^{-2} s^{-1} from a 30 wt. %

$NaBH_4$ solution containing 6.0 M NaOH to a 6.0-M NaOH solution. Choudhury et al. [12] developed a direct borohydride fuel cell employing a poly (vinyl alcohol) hydrogel membrane electrolyte (PHME) and showed that as compared to the Nafion 117 membrane, the crossover rates of $NaBH_4$ through the two membranes were found to be similar. Liu et al. [96] developed a micro borohydride fuel cell that uses a Nafion membrane, and investigated the fuel crossover and its influence on the cathode performance. It was found that the fuel crossover caused a decrease in open-circuit potential on the cathode. Specifically, the use of Pt/C on the cathode showed a potential drop of about 0.11V; while, the use of Ag/C on the cathode showed a potential drop of 0.26 V. In addition, Pt/C was also found to have better stability than Ag/C. It should be mentioned that during the fuel cell operation, the fuel crossover rate was found to decrease due to a decrease in the concentration gradient across the membrane caused by fuel consumption on the anode. Demirci [97] mentioned that for the inhibition of the borohydride anion crossover, the best solution is to develop a highly selective membrane, but it occurs with anion and cation exchange membranes. In summary, the future direction on the borohydride management is to develop the borohydride-impermeable membranes.

4.2. Alkali transport through the membrane (alkali crossover)

Adding an alkali in the fuel solution not only further improves the anodic kinetics, but

also alleviates the hydrolysis of borohydrides. In addition to borohydrides, however, most of the membranes used in this fuel cell system are also permeable to alkali (alkali crossover). The presence of alkali in the cathode, however, will introduce two serious problems [98]. Firstly, the reaction between penetrated alkali and carbon dioxide from the air may cause carbonation precipitation, which has the potential to block some pores of the porous electrode and thus reduce the reaction sites. Secondly, the presence of alkali can also reduce the hydrophobicity of the porous cathode, thereby mismatching the mass transport between water and oxygen. For these reasons, the crossover rate of alkali has to be reduced by using the same strategies that are expected to be effective in lowering the borohydride crossover, such as highly selective membranes [99-106]. For example, Raman et al. [99] developed a direct borohydride/hydrogen peroxide fuel cell that employs a misch-metal alloy anode and a carbon-supported lead sulfate ($PbSO_4$/C) cathode separated with a Nafion 961 membrane. It was found that the use of a Nafion 961 membrane reduced the crossover of sodium hydroxide through the membrane to the cathode, reducing the decomposition rate of hydrogen peroxide and thus increasing the utilization efficiency of hydrogen peroxide. In addition to the crossovered alkali, the alkali is also generated by combining the migrated charge-carrier cations and the produced hydroxide anions in the cathode. Both the crossovered and produced alkali should be removed from the

cathode, which will be discussed in the oxygen transport section.

4.3. Water transport through the membrane (water crossover)

In addition to borohydride and alkali, a significant fraction of liquid water in the fuel solution can transport through the membrane and arrives at the cathode (water crossover). It should be noted that radically different from acid fuel cells, water is a reactant in the ORR process. As such, water transporting through the membrane is essential in an alkaline fuel cell system, but too much water at the cathode may introduce the water flooding problem [95]. Hence, it is a critically important to maintain an appropriate rate of water transport through the membrane. Similarly, water transport through the membrane is also attributed to the three transport mechanisms, i.e., diffusion by the water concentration gradient, EOD by the charge-carrier migration, as well as convection by the liquid pressure gradient. It should be pointed out that the actual fuel cell operation involves the alkali in the fuel solution, meaning that the membrane is always immerged in the alkaline solution, rather than the pure water/water vapor. However, only few investigations on the water transport through the membrane in this fuel cell system was reported in the open literature [42]. Fortunately, the past investigations on the water transport through the membrane in fuel cells have been extensively conducted [107-110], such as alkaline direct alcohol fuel cells. As such, the understandings gained in fuel-electrolyte-fed

fuel cells on the water transport through the membrane can be applied to direct borohydride fuel cells. In summary, the characteristics of water transport through the membrane in this fuel cell system should be addressed in the future.

4.4. Ion transport through the membrane (charge carrier)

In a fuel cell system, charge carriers represent positively or negatively charged ions that form the ionic current by migrating through ion exchange membranes [93]. As mentioned earlier, the cation (typically Na^+) conducting membranes are generally employed in this particular system, as a result of the fact that the use of OH^- conducting membrane causes a serious borohydride-anion crossover problem. As an alkali (typically NaOH) is mixed with borohydride, both anions (OH^-, BH_4^-, BO_2^-) and cations (Na^+/K^+) are presented in the system. It was usually thought that by using Na^+ conducting membrane, the main charge carrier of this fuel cell system was Na^+ ion [95]. Recently, An et al. [93] designed an experimental setup to determine the charge carriers of alkaline direct oxidation fuel cells with the three types of membrane, i.e., anion exchange membrane (Tokuyama A201), cation exchange membrane (Nafion 211), and alkali-doped PBI membrane. It was found that regardless of membranes used, the main charge carrier of three types of membrane was OH^- ion, particularly including the Na^+ conducting membrane. It was also found that the CEM thickness had a strong impact on the distribution of ionic current in this anion-cation

co-existing system. For example, when the thickness of the membrane was increased from 25 μm to 125 μm, the fraction of Na^+ contributing to the ionic current was increased from 30 to 50%. It should be mentioned that the state-of-the-art cation exchange membranes in alkaline media are not a pure cation conductor; hence more attention needs to be paid to enhance the selectivity of cation exchange membranes in this fuel cell system.

5. Transport phenomena in the cathode

5.1. Oxygen transport in the cathode

Like other types of fuel cell, oxygen is transferred from the cathode flow channel through the cathode DL to the cathode CL and then reacts with water and electrons to generate hydroxide ions. The water penetrated from the anode needs to be removed at the cathode [84]. When the water removal rate is too low, the liquid water will accumulate in the cathode and thus lead to a so-called water flooding problem, which lowers the cathode performance. Hence, it is critically important to alleviate the water flooding problem. Typically, there are two operation modes for the oxygen delivery to the reaction sites: active mode [111, 112] and passive mode [113-116]. In passive fuel cells, oxygen is transported to the cathode CL by diffusion and natural convection, while the water removal from the cathode relies on passive forces, such as capillary forces. For this reason, passively accelerating water removal is the key to boost the

cell performance in passive fuel cells. Radically different from the passive one, the removal rate of water can be regulated by the oxygen flow rate in active fuel cells [117-120]. Thus, the gas flow rate plays an important role on the water removal and oxygen transport in active direct borohydride fuel cells. Celik et al. [73] developed a direct borohydride fuel cell using the Pd/C electrocatalyst as anode, the Pt/C electrocatalyst as cathode and Na^+ conducting membrane (Nafion) as the solid electrolyte. They evaluated the cell performance by using the air and oxygen as the oxidant, respectively, in the developed fuel cell system. It was found that as compared to the air, the use of oxygen resulted in a better performance under the same conditions. It was demonstrated that a peak power density of 11.7 mW cm^{-2} was achieved by using oxygen, while the use of the air resulted in a peak power density of 7.3 mW cm^{-2}. In addition, they also found that when the flow rate of the oxidant was increased from 10 mL min^{-1} to 150 mL min^{-1}, the power density was increased from 8.5 mW cm^{-2} to 10.1 mW cm^{-2}. Kim et al. [81] evaluated the power output at different flow rates of fuel and oxidant. The flow rate of the fuel solution was changed from 53 mL min^{-1} to 163.8 mL min^{-1} and the flow rate of the air was changed from 5 L min^{-1} to 10 L min^{-1}. It was found that the maximum peak power density could reach 68 mW cm^{-2} at a current density of 140 mA cm^{-2}, when the flow rates of the fuel solution and the air were 108.4 mL min^{-1} and 10 L min^{-1}, respectively. In addition, they also found

the air humidity was one of the main parameters that could influence the performance of a direct borohydride fuel cell. For example, increasing the air humidity from 65% to 85% resulted in an increase by 11% in the cell performance. It was concluded that the humidification of the air had a positive effect on the removal of sodium hydroxide from the cathode. Similarly, Li et al. [95] constructed a direct borohydride fuel cell that employs a Nafion membrane. It was verified that cations (Na^+) were the charge carrier of the Nafion membrane. The sodium cations will combine the hydroxide anions to form sodium hydroxide in the cathode. For this reason, the alkali produced on the cathode has to be removed together with that crossovered from the anode. Liu et al. [96] suggested that the cathode should be able to efficiently remove the formed NaOH solution, meaning that the cathode should have a balance between the hydrophilic and hydrophobic properties. It was experimentally shown that a wet-proof around 40% would be suitable for the cathode of a direct borohydride fuel cell, because higher and lower wet-proof lead to a smaller limiting current density. In summary, the directions of water/alkali removal and oxygen delivery are opposite, but two processes are intrinsically related to each other. Once water/alkali can be effectively removed, the oxygen will be sufficiently delivered to reaction sites.

5.2. Hydrogen peroxide transport in the cathode

Due to several advantageous characteristics in comparison to gaseous oxygen,

hydrogen peroxide has been widely used as an oxidant in fuel cells, particularly for direct borohydride fuel cells [121-128]. As mentioned earlier, the theoretical voltage of a direct borohydride fuel cell that uses acid/alkaline hydrogen peroxide in the cathode reaches 2.11/3.02 V under the standard condition, which is much higher than that achieved by the conventional fuel cells using oxygen. In addition, the issues associated with the water/alkali removal could be addressed by using hydrogen peroxide, due to the facts that hydrogen peroxide aqueous solution can take away the alkali and water flooding will not be an issue. Thus, many efforts have been devoted to developing direct borohydride fuel cells that use hydrogen peroxide as oxidant and significant progress has been made. For example, Choudhury et al. [61] developed an alkaline direct borohydride fuel cell using hydrogen peroxide as the oxidant and sodium borohydride together with sodium hydroxide as the fuel. They found that when the hydrogen peroxide concertation was changed from 2.23 M to 8.90 M, the effect of hydrogen peroxide concentration on the cell performance is insignificant at low current densities, but became noticeable at high current densities. It was demonstrated that a 4.45-M H_2O_2 operation resulted in a peak power density at temperatures ranging from 30^{o}C and 70^{o}C. They also estimated that the Faradaic efficiency of borohydride oxidation at 70^{o}C was 83%, and the rate of hydrogen evolved at the anode was measured to be 2×10^{-7} mole s^{-1}. Wu et al. [76] investigated

the performance of a direct borohydride fuel cell under different operation conditions, including the electrolyte membrane type, the operating temperature, the borohydride concentration, the supporting electrolyte and the oxidant. It was shown that by using with Pt/C and MnO_2 as anode and cathode electrocatalysts, respectively, as well as the Nafion 117 membrane as the solid electrolyte, when the hydrogen peroxide concentration increased from 1.0 M to 8.0 M, the peak power densities were increased from 1.0 M to 6.0 M and then decreased.

To create a strong alkaline environment, more alkali is also added into the hydrogen peroxide solution [62, 63]. For example, Cao et al. [62] developed an alkaline direct borohydride hydrogen peroxide fuel cell with the Pt-Ru catalyzed nickel foam as anode and the Pd-Ir catalyzed nickel foam as cathode, respectively, via electrodeposition. They investigated the effects of operating parameters, including the borohydride concentration, the hydrogen peroxide concentration, and the operating temperature, on the cell performance. It was found that the fuel cell exhibited an open-circuit voltage (OCV) of 1.0 V and a peak power density of 198 mW cm^{-2} at a current density of 397 mA cm^{-2} when operated with 0.2 M $NaBH_4$ and 3.0 M NaOH as the fuel and 0.4 M H_2O_2 and 3.0 M NaOH as the oxidant at room temperature. Cao et al. [63] prepared the Au catalyzed nickel foam electrodes via spontaneous deposition and investigated electrocatalytic performance for borohydride oxidation

and hydrogen peroxide reduction in the NaOH solution. It was shown that the onset potentials for the borohydride oxidation and hydrogen peroxide reduction were 1.2 V and 0.1 V, respectively. It was found that by using the as-prepared electrodes, the fuel cell exhibited an OCV of 1.07 V and a peak power density of 75 mW cm^{-2} at a current density of 150 mA cm^{-2} when operated with 0.2 M $NaBH_4$ and 2.0 M NaOH as the fuel and 0.5 M H_2O_2 and 2.0 M NaOH as the oxidant at 40°C. They also found that the fuel cell showed higher performance when operated with high-concentration hydrogen peroxide. It should be mentioned that hydrogen peroxide is not stable in strong alkaline environment, chemically and electrochemically decomposing to oxygen and water and thus reducing the utilization efficiency of hydrogen peroxide, as well as degrading the fuel cell performance due to the two-phase counterflow in the cathode. They also found that the rate of decomposition of hydrogen peroxide was faster at higher concentrations. For example, gas evolution occurred in the cathode when the hydrogen peroxide concentration was higher than 0.5 M.

To stabilize the hydrogen peroxide, an acid is generally added into the hydrogen peroxide aqueous solution. For example, Raman et al. [129] developed a direct borohydride fuel cell employing acid hydrogen peroxide as oxidant and found that the peak power density could reach 350 mW cm^{-2} at a cell voltage of 1.2 V at 70°C when operated with 10 wt.% NaOH and 20 wt.% NaOH as the fuel and 15 w/v % H_2O_2

aqueous solution with a pH value of 0 as the oxidant. Wei et al. [67] prepared the carbon-supported Au hollow nanosphere composite electrocatalysts via sacrificial templates at room temperature. By using the as-prepared electrocatalyst, the fuel cell resulted in a peak power density of 25.8 mW cm^{-2} at a current density of 50 mA cm^{-2} when operated at 20^{o}C with the anolyte containing 1.0 M borohydride and 3.0 M sodium hydroxide and the catholyte containing 2.0 M hydrogen peroxide and 0.5 M sulfuric acid. Khadke et al. [66] developed a self-supported direct borohydride-hydrogen peroxide fuel cell system with internal manifolds and an auxiliary control unit and found that it resulted in a peak power of 40 W under ambient conditions. They also investigated the effect of the anolyte and catholyte compositions on the cell performance. For example, when the anolyte composition was kept at 8 wt.% $NaBH_4$ and 11 wt.% NaOH, and the hydrogen peroxide concentration was changed from 6.0 M and 8.0 M in 1.5 M H_2SO_4, the 6.0-M H_2O_2 operation resulted in a better performance due to the increased decomposition rate of hydrogen peroxide at higher concentrations. It should be pointed out that as the theoretical voltage of this system is 3.02 V (the actual voltage is about 2.0 V), there is still plenty of room for the performance to be further upgraded. The large difference between the actual and theoretical voltages is mainly caused by the mixed-potential phenomenon occurring on the cathode, which has been substantially discussed in a

previous review paper [60].

Hydrogen peroxide in the catholyte flowing into the cathode flow channel is transported through the cathode DL to the cathode CL. On the other hand, the chemical and electrochemical decomposition of hydrogen peroxide to oxygen causes oxygen to be removed from the anode CL to the anode flow channel. Like in the anode, therefore, the two-phase counterflow increases the transport resistance of hydrogen peroxide. For this reason, the operating and structural design parameters in the cathode can affect the transportation of hydrogen peroxide from the cathode flow channel to the cathode CL. Similarly, it is also critical to maintain an appropriate hydrogen peroxide concentration in the cathode CL. The factors that can affect the hydrogen peroxide in the cathode CL mainly include the initial hydrogen peroxide concentration, the initial acid concentration, hydrogen peroxide decomposition, as well as structural design parameters, which have been substantially summarized and discussed in previous review papers [46, 60].

6. Concluding remarks

In the past decade, the direct borohydride fuel cell technology has made a rapid progress. This paper reviews the past investigations on transport phenomena in this fuel cell system. Particular attention is paid to the key issues related to the transport of various species through the fuel cell structure. The followings are critical transport

issues that need to be further addressed in the near future.

1) Borohydride management: Minimizing the hydrolysis rate of borohydride and the borohydride-anion crossover rate are the directions to upgrade the cell performance.

2) Alkali management: Alleviating or eliminating the alkali transport through the membrane to the cathode, as well as simultaneously facilitating the alkali removal from the cathode.

3) Water management: Maintaining an appropriate rate of the water transport through the membrane that can match the electrochemical reaction rate at the cathode and simultaneously facilitating the remaining water removal from the cathode.

4) Oxygen management: Enhancing the oxygen delivery to the cathode catalyst layer and simultaneously facilitating the water removal from the cathode diffusion layer by utilizing passive forces or regulating the gas flow rates.

5) Hydrogen peroxide management: Minimizing the decomposition rate of hydrogen peroxide is the direction to upgrade the cell performance.

Acknowledgements

The work described in this paper was supported by a grant from the Natural Science Foundation of China (Project No. 51506039). This work was also conducted under framework of the research and development program of the Korea Institute of Energy Research (B6-2425).

References

[1] Y.S. Li, Y. Feng, X. Sun, Y.L. He, A Sodium-Ion-Conducting Direct Formate Fuel Cell: Generating Electricity and Producing Base, Angew. Chem. 2017 (129) 5828-5831.

[2] L. An, T.S. Zhao, X.L. Zhou, X.H. Yan, C.Y. Jung, A low-cost, high-performance zinc-hydrogen peroxide fuel cell, J. Power Sources 275 (2015) 831-834.

[3] Y.S. Li, Y.L. He, An All-in-One Electrode for High-Performance Liquid-Feed Micro Polymer Electrolyte Membrane Fuel Cells, Journal of The Electrochemical Society 163 (2016) F663-F667.

[4] L. An, R. Chen, Mathematical modeling of direct formate fuel cells, Applied Thermal Engineering, in press.

[5] L. An, L. Zeng, T.S. Zhao, An alkaline direct ethylene glycol fuel cell with an alkali-doped polybenzimidazole membrane, Int. J. Hydrogen Energy 38 (2013) 10602-10606.

[6] S.C. Amendola, P. Onnerud, M.T. Kelly, P.J. Petillo, S.L. Sharp-Goldman, M. Binder, A novel high power density borohydride-air cell, J. Power Sources 84 (1999) 130-133.

[7] J. Ma, Y. Sahai, Cost-effective materials for direct borohydride fuel cells, ECS Trans. 42 (2012) 101-106.

[8] J. Ma, Y. Sahai, R.G. Buchheit, Direct borohydride fuel cell using Ni-based composite anodes, J. Power Sources 195 (2010) 4709-4713.

[9] J. Ma, Y. Sahai, R.G. Buchheit, Evaluation of multivalent phosphate cross-linked chitosan biopolymer membrane for direct borohydride fuel cells, J. Power Sources 202 (2012) 19-27.

[10] N.A. Choudhury, J. Ma, Y. Sahai, High performance and eco-friendly chitosan hydrogel membrane electrolytes for direct borohydride fuel cells, J. Power Sources 210 (2012) 358-365.

[11] J.H. Wee, A comparison of sodium borohydride as a fuel for proton exchange membrane fuel cells and for direct borohydride fuel cells, J. Power Sources 155 (2006) 329-339.

[12] N.A. Choudhury, S.K. Prashant, S. Pitchumani, P. Sridhar, A.K. Shukla, Poly (vinyl alcohol) hydrogel membrane as electrolyte for direct borohydride fuel cells, J. Chem. Sci. 121 (2009) 647-654.

[13] A. Jamaludin, Z. Ahmad, Z.A. Ahmad, A.A. Mohamad, A direct borohydride fuel cell employing a sago gel polymer electrolyte, Int. J. Hydrogen Energy 35 (2010) 11229-11236.

[14] N.A. Choudhury, Y. Sahai, R.G. Buchheit, Chitosan chemical hydrogel electrode binder for direct borohydride fuel cells, Electrochemistry Communications 13 (2011)

1-4.

[15] N.A. Choudhury, J. Ma, Y. Sahai, R.G. Buchheit, High performance polymer chemical hydrogel-based electrode binder materials for direct borohydride fuel cells, J. Power Sources 196 (2011) 5817-5822.

[16] N.A. Choudhury, Y. Sahai, R.G. Buchheit, Polyvinyl alcohol chemical hydrogel electrode binder for direct borohydride fuel cells, J. Electrochem. Soc. 158 (2011) B712-B716.

[17] C. Ponce de León, A. Kulak, S. Williams, I. Merino-Jiménez, F.C. Walsh, Improvemetns in direct borohydride fuel cells using three-dimensional electrodes, Catalysis Today 170 (2011) 148-154.

[18] I. Merino-Jimenez, C. Ponce de León, F.C. Walsh, The effect of surfactants on the kinetics of borohydride oxidation and hydrolysis in the DBFC, Electrochimica Acta 133 (2014) 539–545.

[19] M. Chatenet, F.H.B. Lima, E.A. Ticianelli, Gold is not a Faradaic-efficient borohydride oxidation electrocatalyst: an online electrochemical mass spectrometry study, J. Electrochem. Soc. 157 (2010) B697-B704.

[20] K.S. Freitas, B.M. Concha, E.A. Ticianelli, M. Chatenet, Mass transport effects in the borohydride oxidation reaction-Influence of the residence time on the reaction onset and faradaic efficiency, Catalysis Today 170 (2011) 110-119..

[21] I. Merino-Jimenez, M.J. Janik, C. Ponce de León, F.C. Walsh, Pd-Ir alloy as an anode material for borohydride oxidation, J. Power Sources 269 (2014) 498-508.

[22] Z.P. Li, B.H. Liu, J.K. Zhu, N. Morigasaki, S. Suda, $NaBH_4$ formation mechanism by reaction of sodium borate with Mg and H_2, Journal of Alloys and Compounds 437 (2007) 311-316.

[23] B.H. Liu, Z.P. Li, S. Suda, Influences of alkali in borates on recovery of sodium borohydride, Journal of Alloys and Compounds 474 (2009) L6-L9.

[24] Y. Kojima, T. Haga, Recycling process of sodium metaborate to sodium borohydride, Int. J. Hydrogen Energy 28 (2003) 989-993.

[25] L. Kong, X. Cui, H. Jin, J. Wu, H. Du, T. Xiong, Mechanochemical Synthesis of Sodium Borohydride by Recycling Sodium Metaborate, Energy & Fuels 23 (2009) 5049-5054.

[26] F.H.B. Lima, A.M. Pasqualeti, M.B.M. Concha, M. Chatenet, E.A. Ticianelli, Borohydride electrooxidation on Au and Pt electrodes, Electrochimica Acta 84 (2012) 202-212.

[27] B.M. Concha, M. Chatenet, F. Maillard, E.A. Ticianelli, F.H.B. Lima, R.H.B. Lima, In situ infrared (FTIR) study of the mechanism of the borohydride oxidation reaction, Phys. Chem. Chem. Phys. 12 (2010) 11507-11516.

[28] A.M. Pasqualeti, Pierre-Yves Olu, M. Chatenet, F.H.B. Lima, Borohydride

electrooxidation on carbon-supported noble metal nanoparticles: Insights into hydrogen and hydroxyborane formation, ACS Catalysis 5 (2015) 2778-2787.

[29] Z.P. Li, Z.X. Liu, H.Y. Qin, K.N. Zhu, B.H. Liu, Performance degradation of a direct borohydride fuel cell, J. Power Sources 236 (2013) 17-24.

[30] L.H. Yi, Y.F. Song, W. Yi, X.Y. Wang, H. Wang, P.Y. He, B.A. Hu, Carbon supported Pt hollow nanospheres as anode catalysts for direct borohydride-hydrogen peroxide fuel cells, Int. J. Hydrogen Energy 36 (2011) 11512-11518.

[31] L. An, T.S. Zhao, X.L. Zhou, L. Wei, X.H. Yan, A high-performance ethanol-hydrogen peroxide fuel cell, RSC Advances 4 (2014) 65031-65034.

[32] L. An, T.S. Zhao, R. Chen, Q.X. Wu, A novel direct ethanol fuel cell with high power density, J. Power Sources 196 (2011) 6219–6222.

[33] L. An, T.S. Zhao, Performance of an alkaline-acid direct ethanol fuel cell, Int. J. Hydrogen Energy 36 (2011) 9994-9999.

[34] L. An, T.S. Zhao, L. Zeng, X.H. Yan, Performance of an alkaline direct ethanol fuel cell with hydrogen peroxide as oxidant, Int. J. Hydrogen Energy 39 (2014) 2320-2324.

[35] L. An, T.S. Zhao, Q.X. Wu, L. Zeng, 2012, Comparison of different types of membrane in alkaline direct ethanol fuel cells, Int. J. Hydrogen Energy 37 (2012) 14536-14542.

[36] L. An, R. Chen, Direct formate fuel cells: A review, J. Power Sources 320 (2016) 127-139.

[37] L. An, L. Zeng, T.S. Zhao, An alkaline direct ethylene glycol fuel cell with an alkali-doped polybenzimidazole membrane, Int. J. Hydrogen Energy 38 (2013) 10602-10606.

[38] L. An, Z.H. Chai, L. Zeng, P. Tan, T.S. Zhao, Mathematical modeling of alkaline direct ethanol fuel cells, Int. J. Hydrogen Energy 38 (2013) 14067 -14075.

[39] L. An, T.S. Zhao, Y.S. Li, Carbon-neutral sustainable energy technology: Direct ethanol fuel cells, Renewable and Sustainable Energy Reviews 50 (2015) 1462-1468.

[40] L. An, T.S. Zhao, L. Zeng, Agar chemical hydrogel electrode binder for fuel-electrolyte-fed fuel cells, Applied Energy 109 (2013) 67-71.

[41] U.B. Demirci, P. Miele, Sodium borohydride versus ammonia borane, in hydrogen storage and direct fuel cell applications, Energy Environ. Sci. 2 (2009) 627-637.

[42] S. Lux, L.F. Gu, G. Kopec, R. Bernas, G. Miley, Water management issues for direct borohydride/peroxide fuel cells, J. Fuel Cell Science and Technology 7 (2010) 024501.

[43] B.H. Liu, Z.P. Li, Current status and progress of direct borohydride fuel cell technology development, J. Power Sources 187 (2009) 291-297.

[44] R. Jamard, J. Salomon, A. Martinent-Beaumont, C. Coutanceau, Life time test in direct borohydride fuel cell system, J. Power Sources 193 (2009) 779-787.

[45] I. Merino-Jiménez, C. Ponce de León, A.A. Shah, F.C. Walsh, Developments in direct borohydride fuel cells and remaining challenges, J. Power Sources 219 (2012) 339-357.

[46] J. Ma, N.A. Choudhury, Y. Sahai, A comprehensive review of direct borohydride fuel cells, Renewable and Sustainable Energy Reviews 14 (2010) 183-199.

[47] V. Kiran, S. Srinivasan, A short review on direct borohydride fuel cells, J. Indian Institute of Science 89 (2009) 447-454.

[48] C. Ponce de León , F.C. Walsh, D. Pletcher, D.J. Browning, J.B. Lakeman, Direct borohydride fuel cells, J. Power Sources 155 (2006) 172-181.

[49] J.H. Wee, Which type of fuel cell is more competitive for portable application: Direct methanol fuel cells or direct borohydride fuel cells?, J. Power Sources 161 (2006) 1-10.

[50] C. Ponce de León, F.C. Walsh, R.R. Bessette, C.J. Patrissi, M.G. Medeiros, A. Rose, D. Browning, J.B. Lakeman, R.W. Reevec, Recent developments in borohydride fuel cells, ECS Transactions 15 (2008) 25-49.

[51] L. An, T.S. Zhao, An alkaline direct ethanol fuel cell with a cation exchange membrane, Energy Environ. Sci. 4 (2011) 2213-2217.

[52] Z.P. Li, B.H. Liu, K. Arai, S. Suda, A fuel cell for using borohydrides as the fuel, J. Electrochem. Soc. 150 (2003) A868-A872.

[53] Y.S. Li, Y.L. He, W.W. Yang, A high-performance direct formate-peroxide fuel cell with palladium-gold alloy coated foam electrodes, J. Power Sources 278 (2015) 569-573.

[54] Y.S. Li, H. Wu, Y. Liu, L. Jin, Performance of direct formate-peroxide fuel cells, J. Power Sources 287 (2015) 75-80.

[55] Y.S. Li, X. Sun, Y. Feng, Hydroxide Self-Feeding High-Temperature Alkaline Direct Formate Fuel Cells, ChemSusChem 10 (2017) 2135-2139.

[56] L. An, R. Chen, Recent progress in alkaline direct ethylene glycol fuel cells for sustainable energy production, J. Power Sources 329 (2016) 484-501.

[57] L. An, T.S. Zhao, Z.H. Chai, L. Zeng, P. Tan, Modeling of the mixed potential in hydrogen peroxide-based fuel cells, Int. J. Hydrogen Energy 39 (2014) 7407-7416.

[58] L. An, T.S. Zhao, Transport phenomena in alkaline direct ethanol fuel cells for sustainable energy production, J. Power Sources 341 (2017) 199-211.

[59] L. An, T.S. Zhao, Z.H. Chai, P. Tan, L. Zeng, Mathematical modeling of an anion-exchange membrane water electrolyzer for hydrogen production, Int. J. Hydrogen Energy 39 (2014) 19869-19876.

[60] L. An, T.S. Zhao, X.H. Yan, X.L. Zhou, P. Tan, The dual role of hydrogen

peroxide in fuel cells, Science Bulletin 60 (2015) 55-64.

[61] N.A. Choudhury, R.K. Raman, S. Sampath, A.K. Shukla, An alkaline direct borohydride fuel cell with hydrogen peroxide as oxidant, J. Power Sources 143 (2005) 1-8.

[62] D.X. Cao, D.D. Chen, J. Lan, G.L. Wang, An alkaline direct NaBH4-H2O2 fuel cell with high power density, J. Power Sources 190 (2009) 346-350.

[63] D.X. Cao, Y.Y. Gao, G.L. Wang, R.R. Miao, Y. Liu, A direct NaBH4-H2O2 fuel cell using Ni foam supported Au nanoparticles as electrodes, Int. J. Hydrogen Energy 35 (2010) 807-813.

[64] Z.P. Li, B.H. Liu, K. Arai, K. Asaba, S. Suda, Evaluation of alkaline borohydride solutions as the fuel for fuel cell, J. Power Sources 126 (2004) 28-33.

[65] N. Duteanu, G. Vlachogiannopoulos, M.R. Shivhare, E.H. Yu, K. Scott, A parametric study of a platinum ruthenium anode in a direct borohydride fuel cell, J. Appl Electrochem 37 (2007) 1085-1091.

[66] P.S. Khadke, P. Sethuraman, P. Kandasamy, S. Parthasarathi, A.K. Shukla, A self-supported direct borohydride-hydrogen peroxide fuel cell system, Energies 2 (2009) 190-201.

[67] J.L. Wei, X.Y. Wang, Y. Wang, J. Guo, P.Y. He, S.Y. Yang, N. Li, F. Pei, Y.S. Wang, Carbon-supported Au hollow nanospheres as anode catalysts for direct

borohydride-hydrogen peroxide fuel cells, Energy & Fuels 23 (2009) 4037-4041.

[68] H.J. Wu, C. Wang, Z.X. Liu, Z.Q. Mao, Influence of operation conditions on direct $NaBH_4/H_2O_2$ fuel cell performance, Int. J. Hydrogen Energy xxx (2009) 1-4.

[69] D.X. Cao, Y.Y. Gao, G.L. Wang, R.R. Miao, Y. Liu, A direct NaBH4-H2O2 fuel cell using Ni foam supported Au nanoparticles as electrodes, Int. J. Hydrogen Energy 35 (2010) 807-813.

[70] C. Celik, F.G.B. San, H.I. Sarac, Influences of sodium borohydride concentration on direct borohydride fuel cell performance, J. Power Sources 195 (2010) 2599-2603.

[71] D.M.F. Santos, P.G. Saturnino, R.F.M. Lobo, C.A.C. Sequeira, Direct borohydride/peroxide fuel cells using Prussian Blue cathodes, J. Power Sources 208 (2012) 131-137.

[72] W. Jin, J.G. Liu, Y.T. Wang, Y.F. Yao, J. Gu, Z.G. Zou, Direct NaBH4-H2O2 fuel cell based on nanoporous gold leaves, Int. J. Hydrogen Energy 38 (2013) 10992-10997.

[73] C. Celik, F.G.B. San, H.I. Sarac, Effects of operation conditions on direct borohydride fuel cell performance, J. Power Sources 185 (2008) 197-201.

[74] H. Cheng, K. Scott, Influence of operation conditions on direct borohydride fuel cell performance, J. Power Sources 160 (2006) 407-412.

[75] D.M.F. Santos, J.A.D. Condeço, M.W. Franco, C.A.C. Sequeira, An improved

borohydride-H2O2 laboratory fuel cell, ECS Transactions 3 (2007) 19-30.

[76] H.J. Wu, C. Wang, Z.X. Liu, Z.Q. Mao, Influence of operation conditions on direct NaBH4/H2O2 fuel cell performance, Int. J. Hydrogen Energy 35 (2010) 2648-2651.

[77] H.Y. Qin, Z.X. Liu, Y.F. Guo, Z.P. Li, The effects of membrane on the cell performance when using alkaline borohydride-hydrazine solutions as the fuel, Int. J. Hydrogen Energy 35 (2010) 2868-2871.

[78] C. Celik, F.G.B. San, H.I. Sarac, Improving the direct borohydride fuel cell performance with thiourea as the additive in the sodium borohydride solution, Int. J. Hydrogen Energy 35 (2010) 8678-8682.

[79] C. Gabrielli, F. Huet, R.P. Nogueira, Fluctuations of concentration overpotential generated at gas-evolving electrodes, Electrochimica Acta 50 (2005) 3726-3736.

[80] H.Y. Qin, Z.X. Liu, W.X. Yin, J.K. Zhu, Z.P. Li, Effects of hydrazine addition on gas evolution and performance of the direct borohydride fuel cell, J. Power Sources 185 (2008) 895-898.

[81] C. Kim, K.J. Kim, M.Y. Ha, Performance enhancement of a direct borohydride fuel cell in practical running conditions, J. Power Sources 180 (2008) 154-161.

[82] B.H. Liu, Z.P. Li, J.K. Zhu, S. Suda, Influences of hydrogen evolution on the cell and stack performances of the direct borohydride fuel cell, J. Power Sources 183

(2008) 151-156.

[83] Z.P. Li, B.H. Liu, J.K. Zhu, S. Suda, Depression of hydrogen evolution during operation of a direct borohydride fuel cell, J. Power Sources 163 (2006) 555-559.

[84] T.S. Zhao, C. Xu, R. Chen, W.W. Yang, Mass transport phenomena in direct methanol fuel cells, Progress in Energy and Combustion Science 35 (2009) 275–292.

[85] X. Li, I. Sabir, Review of bipolar plates in PEM fuel cells: Flow-field designs, Int. J. Hydrogen Energy 30 (2005) 359-371.

[86] C. Xu, T.S. Zhao, A new flow field design for polymer electrolyte-based fuel cells, Electrochem. Commun. 9 (2007) 497-503

[87] Y.K. Zeng, X.L. Zhou, L. An, L. Wei, T.S. Zhao, A high-performance flow-field structured iron-chromium redox flow battery, J. Power Sources 324 (2016) 738-744.

[88] G. Miley, B. Bernas, K.J. Kim, N. Luo, Optimization of catalyst deposited diffusion layer for a direct sodium borohydride fuel cell (DNBFC), ECS Transactions 17 (2009) 525-542.

[89] L.F. Gu, N. Luo, G.H. Miley, Cathode electrocatalyst selection and deposition for a direct borohydride/hydrogen peroxide fuel cell, J. Power Sources 173 (2007) 77-85.

[90] H. Cheng, K. Scott, Investigation of Ti mesh-supported anodes for direct borohydride fuel cells, J. Applied Electrochemistry 36 (2006) 1361-1366.

[91] F. Yang, K. Cheng, Y.H. Mo, L.Q. Yu, J.J. Yin, G.L. Wang, D.X. Cao, Direct

peroxide-peroxide fuel cell - Part 1: The anode and cathode catalyst of carbon fiber cloth supported dendritic Pd, J. Power Sources 217 (2012) 562-568.

[92] F. Yang, K. Cheng, X.L. Liu, S. Chang, J.J. Yin, C.Y. Du, L. Du, G.L. Wang, D.X. Cao, Direct peroxide-peroxide fuel cell - Part 2: Effects of conditions on the performance, J. Power Sources 217 (2012) 569-573.

[93] L. An, T.S. Zhao, Y.S. Li, Q.X. Wu, Charge carriers in alkaline direct oxidation fuel cells, Energy & Environmental Science 5 (2012) 7536-7538.

[94] B.H. Liu, S. Suda, Influences of fuel crossover on cathode performance in a micro borohydride fuel cell, J. Power Sources 164 (2007) 100-104.

[95] Y.S. Li, T.S. Zhao, R. Chen, Cathode flooding behavior in alkaline direct ethanol fuel cells, J. Power Sources 196 (2011) 133-139.

[96] B.H. Liu, S. Suda, Influences of fuel crossover on cathode performance in a micro borohydride fuel cell, J. Power Sources 164 (2007) 100-104.

[97] U.B. Demirci, Direct borohydride fuel cell: Main issues met by the membrane-electrodes-assembly and potential solutions, J. Power Sources 172 (2007) 676-687.

[98] T.S. Zhao, Y.S. Li, S.Y. Shen, Anion-exchange membrane direct ethanol fuel cells: Status and perspective, Front. Energy Power Eng. China 4 (2010) 443-458.

[99] R.K. Raman, A.K. Shukla, A direct borohydride/hydrogen peroxide fuel cell with

reduced alkali crossover, Fuel Cells 7 (2007) 225-231.

[100] H. Cheng, K. Scott, K.V. Lovell, J.A. Horsfall, S.C. Waring, Evaluation of new ion exchange membranes for direct borohydride fuel cells, J. Membrane Science 288 (2007) 168-174.

[101] Y.G. Wang, P. He, H.S. Zhou, A novel direct borohydride fuel cell using an acid-alkaline hybrid electrolyte, Energy Environ. Sci. 3 (2010) 1515-1518.

[102] D.M.F. Santos, C.A.C. Sequeira, Polymeric membranes for direct borohydride fuel cells: a comparative study, ECS Transactions 25 (2010) 111-122.

[103] J. Ma, N.A. Choudhury, Y. Sahai, R.G. Buchheit, A high performance direct borohydride fuel cell employing cross-linked chitosan membrane, J. Power Sources 196 (2011) 8257-8264.

[104] X.D. Yang, Y.N. Liu, S. Li, X.Z. Wei, L. Wang, Y.Z. Chen, A direct borohydride fuel cell with a polymer fiber membrane and non-noble metal catalysts, Scientific Reports 2 (2012) 1-5.

[105] R.W. Reeve, A sodium borohydride - hydrogen peroxide fuel cell employing a bipolar membrane electrolyte, ECS Transactions 42 (2012) 117-129.

[106] D.M.F. Santos, C.A.C. Sequeira, Effect of membrane separators on the performance of direct borohydride fuel cells, J. Electrochem. Soc. 159 (2011) B126-B132.

[107] Q.X. Wu, T.S. Zhao, R. Chen, W.W. Yang, Effects of anode microporous layers made of carbon powder and nanotubes on water transport in direct methanol fuel cells, J. Power Sources 191 (2009) 304-311.

[108] X.H. Wang, J.P. McClure, P.S. Fedkiw, Transport properties of proton- and hydroxide-exchange membranes for fuel cells, Electrochim. Acta 79 (2012) 126-132.

[109] Q.J. Duan, S.H. Ge, C.Y. Wang, Water uptake, ionic conductivity and swelling properties of anion-exchange membrane, J. Power Sources 243 (2013) 773-778.

[110] T.S. Zhao, R. Chen, W.W. Yang, C. Xu, Small direct methanol fuel cells with passive supply of reactants, J. Power Sources 191 (2009) 185–202.

[111] H. Cheng, K. Scott, K. Lovell, Material aspects of the design and operation of direct borohydride fuel cells, Fuel Cells 6 (2006) 367-375.

[112] R. Jamard, A. Latour, J. Salomon, P. Capron, A. Martinent-Beaumont, Study of fuel efficiency in a direct borohydride fuel cell, J. Power Sources 176 (2008) 287-292.

[113] B.H. Liu, Z.P. Li, K. Arai, S. Suda, Performance improvement of a micro borohydride fuel cell operating at ambient conditions, Electrochimica Acta 50 (2005) 3719-3725.

[114] B.H. Liu, Z.P. Li, S. Suda, A study on performance stability of the passive direct borohydride fuel cell, J. Power Sources 185 (2008) 1257-1261.

[115] J.F. Ma, Y.N. Liu, Design of a membraneless passive planar four-cell direct

borohydride fuel cell, J. Fuel Cell Science and Technology 9 (2012) 011004-1-3.

[116] B.H. Liu, Z.P. Li, S. Suda, Development of high-performance planar borohydride fuel cell modules for portable applications, J. Power Sources 175 (2008) 226-231.

[117] Z.P. Li, B.H. Liu, K. Arai, S. Suda, Development of the direct borohydride fuel cell, J. Alloys and Compounds 404-406 (2005) 648-652.

[118] S. Towne, M. Carella, W.E. Mustain, V. Viswanathan, P. Rieke, U. Pasaogullari, P. Singh, Performance of a direct borohydride fuel cell, ECS Transactions 25 (2009) 1951-1957.

[119] D.M.F. Santos, C.A.C. Sequeira, Sodium borohydride as a fuel for the future, Renewable and Sustainable Energy Reviews 15 (2011) 3980-4001.

[120] J.S. Park, S.H. Park, S.D. Yim, Y.G. Yoon, W.Y. Lee, C.S. Kim, Performance of solid alkaline fuel cells employing anion-exchange membranes, J. Power Sources 178 (2008) 620-626.

[121] J.L. Wei, X.Y. Wang, Y. Wang, J. Guo, P.Y. He, S.Y. Yang, N. Li, F. Pei, Y.S. Wang, Carbon-supported Au hollow nanospheres as anode catalysts for direct borohydride-hydrogen peroxide fuel cells, Energy & Fuels 23 (2009) 4037-4041.

[122] J. Ma, Y. Sahai, R.G. Buchheit, Direct borohydride fuel cell using Ni-based composite anodes, J. Power Sources 195 (2010) 4709-4713.

[123] G. Selvarani, S.K. Prashant, A.K. Sahu, P. Sridhar, S. Pitchumani, A.K. Shukla, A direct borohydride fuel cell employing Prussian Blue as mediated electron-transfer hydrogen peroxide reduction catalyst, J. Power Sources 178 (2008) 86-91.

[124] V.W.S. Lam, D.C.W. Kannangara, A. Alfantazi, E.L. Gyenge, Electrodeposited osmium three-dimensional anodes for direct borohydride fuel cells, J. Power Sources 212 (2012) 57-65.

[125] N. Luo, G.H. Miley, R. Gimlin, R. Burton, J. Rusek, F. Holcomb, Hydrogen-peroxide-based fuel cells for space power systems, J. Propulsion and Power 24 (2008) 583-589.

[126] N. Luo, G.H. Miley, K.J. Kim, R. Burton, X.Y. Huang, NaBH4/H2O2 fuel cells for air independent power systems, J. Power Sources 185 (2008) 685-690.

[127] M. Romer, G.H. Miley, N. Luo, R. Gimlin, Ragone Plot comparison of radioisotope cells and the direct sodium borohydride/hydrogen peroxide fuel cell with chemical batteries, IEEE Transactions on Energy Conversion 23 (2008) 171-178.

[128] A.E. Sanli, M.L. Aksu, B.Z. Uysal, Advanced mathematical model for the passive direct borohydride/peroxide fuel cell, Int. J. Hydrogen Energy 36 (2011) 8542-8549.

[129] R.K. Raman, N.A. Choudhury, A.K. Shukla, A high output voltage direct borohydride fuel cell, Electrochemical and Solid-State Letters 7 (2004) A488-A491.

Figure captions:

Fig. 1 Schematics of an alkaline direct borohydrides fuel cell using: (a) an anion exchange membrane; (b) a cation exchange membrane.

Fig. 2 Schematic of an alkaline direct borohydrides fuel cell operating with hydrogen peroxide as oxidant [61].

Fig. 3 (a) Effect of the borohydride concentration on the cell performance [62]; (b) effect of the alkali concentration on the cell performance [64].

Fig. 4 Effect of the additive on (a) the gas evolution and (b) the cell performance [80].

Fig. 5 (a) Visualization photo of anode channel when active hydrogen generation occurs; (b) photograph of anode when hydrogen bubbles are held in narrow gap between anode and acrylic end-plate; (c) Photograph of corrugated anode [81].

Fig. 6 (a) Direct borohydride fuel cell stack measurement set-up; (b) fuel supplies in the 20-cell stack: (left) parallel supply and (right) divided parallel supply [82].

Fig. 7 Flow fields: (a) serpentine (SFF) and (b) parallel (PFF) [74].

Fig. 8 (a) SEM image of Au deposits using electrodeposition method; (b) SEM image of Au deposits using sputtering method; (c) V-I and P-I curves generated by electrodeposited gold catalyst layer and electrodeposited palladium layer at 60°C [89].

Highlights

- Past research on transport phenomena in DBFCs is reviewed.
- Particular attention is paid to transport issues in DBFCs.
- Some future perspectives are also highlighted.

Graphical Abstract: This article provides a comprehensive review of transport phenomena in direct borohydrides fuel cells.